GUI-Based AC Induced Corrosion Monitoring for Buried Pipelines near HVTLs

Kazeem B. Adedeji, *Member, IAENG,* Akinlolu A. Ponnle, Bolanle T. Abe, *Member, IAENG,* Adisa A. Jimoh, Adnan M. Abu-Mahfouz and Yskandar Hamam, *Member, IAENG*

***Abstract*—In this paper, a stand-alone application with graphical user interface (GUI) developed for monitoring AC induced corrosion expectancies of buried pipelines near a high voltage AC transmission line is presented. A Rand water site, South Africa, was used as a case study. The interface was based on estimating the AC induced corrosion risk assessment indices for buried pipelines near existing overhead high voltage transmission lines using Carson's concept of mutual impedances between both the pipeline and transmission circuits. The GUI was developed using MATLAB software and have been tested to process user input data from field measurements in such site. The developed application permits the evaluation of the AC induced corrosion risk assessment indices and may be particularly useful in the analysis of AC induced potential on buried pipelines.**

***Index Terms*—AC assisted corrosion, AC corrosion assessment criteria, graphical user interface, high voltage transmission lines, pipelines.**

I. Introduction

THE interference from overhead high voltage power transmission lines (HVTLs) on metallic pipelines in the same utility corridor has posed a serious threat to owners of pipelines around the world and has attracted the attention of many researchers in recent years. Increasing energy demand and the cost of right-of-way suitable for pipelines and transmission lines, coupled with land use regulations [1], has forced organizations to a situation whereby their pipelines and transmission lines have to follow the same route. The number of situations is on the increase where new pipelines have to be installed next to existing HVTLs. Consequently, the current flowing through the transmission line phase conductors produces a time varying electromagnetic field which couples to any metallic pipelines in its right-of-way, resulting in an induced voltage on the pipeline. It should, however, be noted that the induced voltage may occur during both steady-state and transient condition of the transmission lines [2, 3]. Thereafter, the induced voltage causes current circulation between the pipeline and the surrounding soil through the pipeline coating defect [4–6]. This leads to accelerated corrosion at the precise point where stray current leaves the pipeline during the current circulation. Asides causing accelerated corrosion, the safety of personnel working on the pipeline is crucial because an appreciable voltage magnitude could be impressed on the pipeline due to transmission line fault [1, 7–9]. The pipeline materials and its coating may also be compromised leading to high cost of maintenance and repairs most especially for buried pipelines. Therefore, the National Association of Corrosion Engineer (NACE) recommended that for safety of personnel working on the pipeline, the steady state induced potential should be considered dangerous and be mitigated if the measured or estimated potential on the pipeline exceeds 15 $Vr.m.s$ [10].

AC induced corrosion problem has been examined by many researchers and scientific organizations leading to various research reports and technical standards. Of particular interest is the technical specification and threshold values provided on the criteria for assessing AC induced corrosion of pipelines [11–15]. These values are based on the practical experience in the field of AC corrosion. One of the generally accepted ways of assessing corrosion risk due to AC is to monitor the variation in the AC density through the pipeline coating defect [5, 12–23]. These research studies revealed that AC density between 30 and 100 A/m^2 translates to the occurrence of AC corrosion on pipelines while a value in excess of 100 A/m^2 amounts to corrosion damage likelihood [11, 13]. Other AC induced corrosion assessment criteria reported in literature include pipe-to-soil potential and relative risk value of AC corrosion measured along the length of the parallel exposure of the pipeline with the transmission lines [13, 15]. It was stipulated that in order to reduce the corrosion likelihood on pipelines near transmission lines, the measured/estimated pipe-to-soil potential should at any time not exceed 4 V where the soil resistivity is less than 25 $\Omega.m$, and 10 V where the soil resistivity is greater than 25 $\Omega.m$ [13]. The assessment criteria based on the relative risk (RR) value of AC induced corrosion along the length of the pipe was proposed by Philip [15]. This criterion was based on the measurement of the pipe-to-soil potential and the immediate soil resistivity in which the pipe is buried. An RR value in excess of 0.22 translates to the occurrence of AC corrosion expectancy, thereby prompting for the installation of a mitigation technique. Therefore, these AC induced corrosion risk assessment criteria may be used to predict corrosion progress on pipelines. In general, in areas where these limits are exceeded, and AC corrosion is suspected, the AC corrosion assessment criteria must be monitored from time to time and AC induced mitigation system installed.

For AC assisted corrosion to be monitored on pipelines, it requires a constant measurement of these AC corrosion assessment criteria. However, measuring the pipe-to-soil potential along the exposed length of the pipeline is a very challenging task and requires huge human involvements. Fig. 1 shows a practical way of measuring the pipe-to-soil

Manuscript received April 16, 2018, revised July 04, 2018.
This work was supported by the Tshwane University of Technology, Pretoria, South Africa and the Rand Water, South Africa.

The authors are with the Department of Electrical Engineering, Tshwane University of Technology, Pretoria South Africa.

A.A. Ponnle is also with the Department of Electrical and Electronics Engineering, Federal University of Technology, Akure, Ondo State, Nigeria.

A.M. Abu-Mahfouz is also with Meraka Institute, CSIR, Pretoria, South Africa.

Y. Hamam is also an Emeritus Professor, ESIEE-Paris, France.

Corresponding author: Adedeji K.B., Email: adedejikb@tut.ac.za.

potential along the length of a buried pipeline.

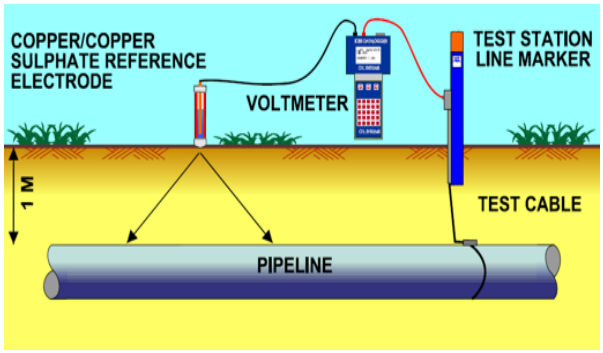

Fig. 1. A practical way of measuring the pipe-to-soil potential.

As shown in the figure, assuming the pipeline is buried far beneath the soil and this measurement is to be conducted at different points along the length of the pipeline, it demands a tedious task. Consequently, a simulation tool may provide a better option in this regard and for corrosion prediction due to AC. Some simulation tools have been developed in the past and recent time for AC induced interference analysis [24–27]. These tools such as the right-of-way module of the current distribution electromagnetic field, grounding and soil structure analysis (CDGES) developed by the SES Technology, Canada [26], are mostly used for simulating the induced voltage on pipeline near a power transmission line. However, to the knowledge of the authors, other AC corrosion assessment (AC density and relative risk of AC corrosion) have not been integrated into these tools and most are not open-source. In this paper, a stand-alone computer application with GUI incorporating these AC assisted corrosion criteria developed to assess and predict AC induced corrosion based on these criteria is presented. Although, this work is only adapted for the case study site at Strydpan in South Africa, future work is ongoing to improve its flexibility for adaptation to any pipeline and HVTL configuration.

II. Research Methods

The graphical user interface (GUI) for the pipeline AC induced corrosion risk assessment for the Rand Water, Strydpan site, South Africa, was developed in the MATLAB environment, and has been made to run as a standalone executable program using the *deployment tool* in MATLAB. As stated in earlier Section, the GUI was developed to assess and monitor the AC corrosion expectancies of a water pipeline buried near an existing power transmission line in the above mentioned site. And before the description of the GUI, an overview of the study site and the evaluation of the corrosion risk assessment criteria is first presented.

A. Network of the HVTL and pipeline description

Fig. 2 illustrates the schematic diagram of the transmission lines and pipeline model ROW. As may be seen in Fig. 2, the system consists of four single circuit 275 kV HVTLs in a horizontal configuration (with two overhead earth wires on each tower) and a water pipeline buried at a depth h_p beneath the soil surface. The pipe has a radius r_p and it is coated with polyethylene polymer with a thickness t_c. Also, the pipe runs parallel to the HVTLs for a length L. The transmission lines tower dimension, configurations and the coordinates on the pipe across the ROW are depicted in Fig. 2. The transmission lines were evenly spaced at a tower centre to centre distance of 32 m from each other.

B. Induced AC voltage analysis

Consider a single-circuit overhead line with k^{th} earth wire, each current in the phase conductors induces a voltage on the pipeline through the appropriate mutual impedance between the pipeline and the conductor. The longitudinal electromotive force (LEF) E_p induced on the pipeline due to the three-phase currents I_R, I_W, I_B and the earth wire current may be expressed as

$$E_p = I_R Z_{R-p} + I_W Z_{W-p} + I_B Z_{B-p} - \sum_{k=1}^{n} I_{gk} Z_{gk-p} \quad (1)$$

where I_R, I_W, I_B and I_{gk} are the steady state currents in the phase conductors and the k^{th} earth wires, and Z_{R-p}, Z_{W-p}, Z_{B-p}, Z_{gk-p} are the mutual impedances (Ω/m) between the phase conductors, the k^{th} earth wire and the pipeline, n represents the number of earth wires on the tower. If the potential drop across the k^{th} earth wire due to the effect of the phase conductors is represented by V_{gk} and the currents in the earth wires by $I_{gk} = \frac{Vgk}{Z_{ggk}}$, where Z_{ggk} denotes the self-impedance of the k^{th} earth wire, thus, after further simplification, the longitudinal EMF induced on the pipeline due to the coupling effect of the i^{th} transmission line may be expressed as

$$\begin{aligned} E_{p_i} = {} & I_{R_i}\left(Z_{R_i-p} - \sum_{k=1}^{n} \frac{Z_{R_i-gk} Z_{gk-p}}{Z_{ggk}}\right) \\ & + I_{W_i}\left(Z_{W_i-p} - \sum_{k=1}^{n} \frac{Z_{W_i-gk} Z_{gk-p}}{Z_{ggk}}\right) \\ & + I_{B_i}\left(Z_{B_i-p} - \sum_{k=1}^{n} \frac{Z_{B_i-gk} Z_{gk-p}}{Z_{ggk}}\right) \end{aligned} \quad (2)$$

In (2), i is an integer ranging from $1, 2, , N$. N represents the number of transmission line (N=4 for the current study). Also, I_{R_i}, I_{W_i} and I_{B_i} denote the steady-state currents in the phase conductors of the i^{th} transmission line, Z_{R_i}, Z_{W_i} and Z_{B_i} are the mutual impedances between the R-W-B phase conductors of the i^{th} transmission line and the pipe. It is important to mention that the steady-state current in each of the phase conductors (I_{R_i}, I_{W_i} and I_{B_i}) is alternating with a phase angle of 120^0, 0, -120^0 to each other.

The mutual impedance between two circuits with earth return, for example, a pipe p and an overhead transmission line phase conductor R, W, B or earth wire conductor g, or between the earth wire and the phase conductors may be evaluated using (3)

$$Z_{p-m} = \frac{\omega \mu_o}{8} + j\left(\frac{\omega \mu_o}{2\pi} log_e\left[\frac{\delta_e}{D_{p-m}}\right]\right) \quad \forall m \epsilon (R, W, B, g_{k-i}) \quad (3)$$

where μ_o denotes the magnetic permeability of free space, ω is the angular frequency of the transmission line, δ_e denotes the depth of equivalent earth return and D_{p-m} is the geometric mean distances (GMDs) linking each of the

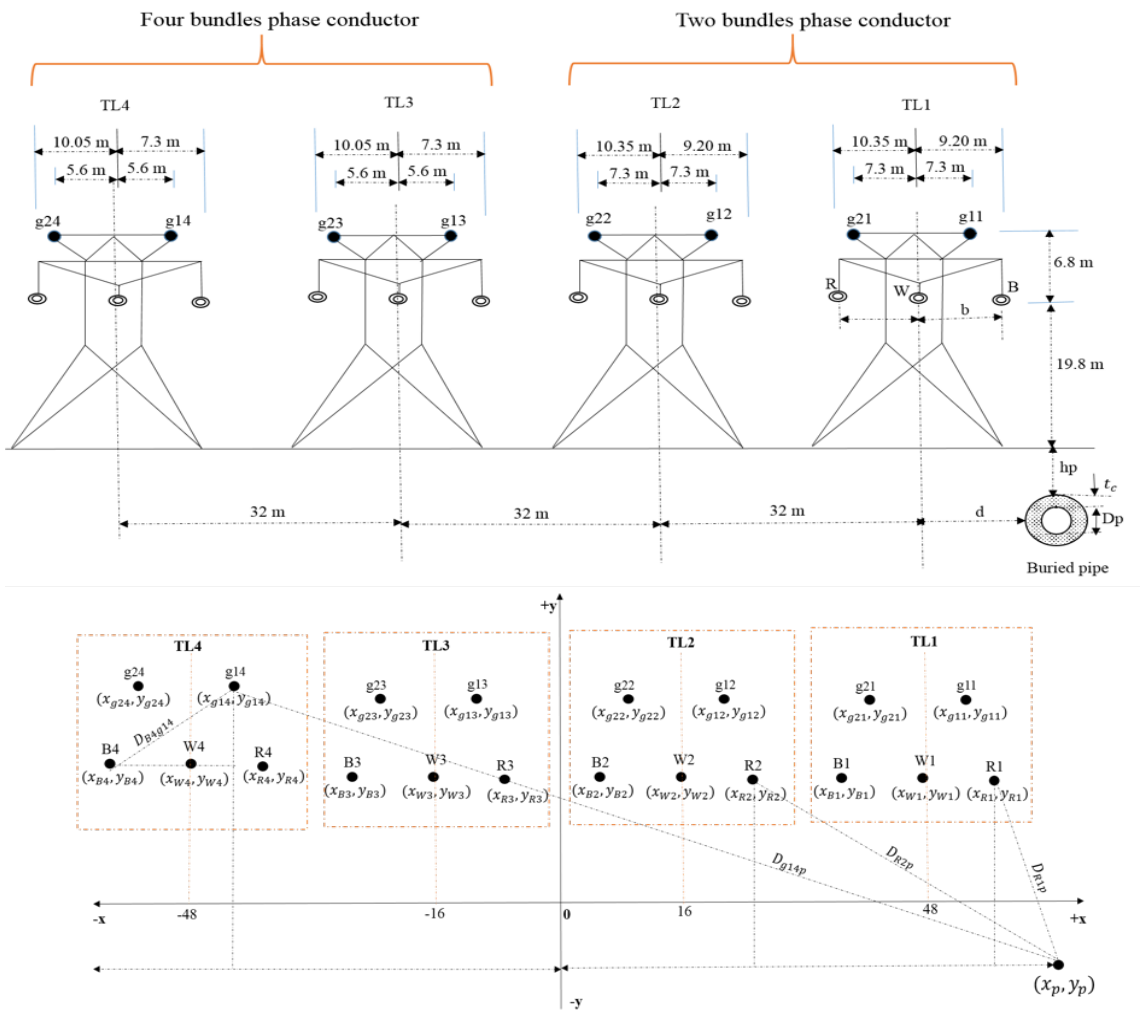

Fig. 2. The case study site (a) schematics of the HVTL-pipeline ROW for the study site (b) coordinates of the HVTL-pipeline ROW for the study site.

$R-W-B$ or gk conductors and the pipeline or between the $R-W-B$ phase conductors and the k^{th} earth wire. Also, the self-impedance of the earth wire conductors with earth return may be expressed as

$$Z_{ggk} = R_{gk} + \frac{\omega\mu_o}{8} + j\left(\frac{\omega\mu_o}{2\pi}\left[\frac{1}{4} + log_e\left[\frac{\delta_e}{R_{GM_k}}\right]\right]\right) \quad (4)$$

In (4), R_{gk} represents the AC resistance of the k^{th} earth wire and R_{GM_k} denotes the geometric mean radius of the k^{th} earth wire conductors. The nominal values of R_{gk} and R_{GM_k} depend on the type of earth wire used, the values of which are provided by the manufacturer. Alternatively, the R_{gk} may be estimated using

$$R_{gk} = \frac{\rho_e l}{A_{eff}} \quad (5)$$

where ρ_e represents the resistivity of the earth wire, l is the length of the conductor and A_{eff} its the effective cross-sectional area. The depth of equivalent earth return δ_e is related to the soil resistivity ρ_{soil} and the transmission line operating frequency f as

$$\delta_e = 658.87\sqrt{\frac{\rho_{soil}}{f}} \quad (6)$$

The D_{p-m} in (3) may be estimated by applying Pythagoras' theorem to the transmission line/pipeline coordinates shown in Fig. 2(b) as

$$D_{p-m} = \sqrt{(x_p - x_m)^2 + (y_m - y_p)^2},\ \forall m \epsilon (R, W, B, g_{k-i}) \quad (7)$$

where x_p represents the horizontal position of the pipe across the transmission line ROW, y_p represents the pipe depth from the ground to the centre of the pipe. It should be noted that $y_p = (h_p + r_p + t_c)$ as in Fig. 2(a). Also, $y_m \forall m \epsilon (R, W, B, g_{k-i})$ represents the various heights of the phase conductors or the earth wire from the ground surface while their horizontal position may be represented by $x_m \forall m \epsilon (R, W, B, g_{k-i})$ on the x-coordinate.

The longitudinal induced EMF (V/m) on the pipe, E_p, is computed as the resultant of the individual inductive coupling effects of the N transmission lines. Thus

$$E_p = \sum_{i=1}^{N=4} E_{p_i} \quad (8)$$

Therefore, the longitudinal induced voltage (V) on the entire pipeline exposure length L may be computed as

$$V_p = E_p L \quad (9)$$

C. Evaluation of the pipe-to-soil-potential

To estimate the pipe-to-soil potential at any point x, along the parallel length of the pipeline, a circuit analysis method is applied to the pipe-transmission line equivalent circuit. To this end, the pipeline was modelled as a lossy transmission line having a series impedance and a shunt admittance together with a distributed voltage source which is equivalent to the longitudinal induced EMF on the pipeline. The equivalent circuit diagram of a distributed pipeline section of length L in parallel with an overhead HVTL is shown in Fig. 3. In this figure, the pipeline has a termination impedances of Z_1 and Z_2 seen from ends A and B.

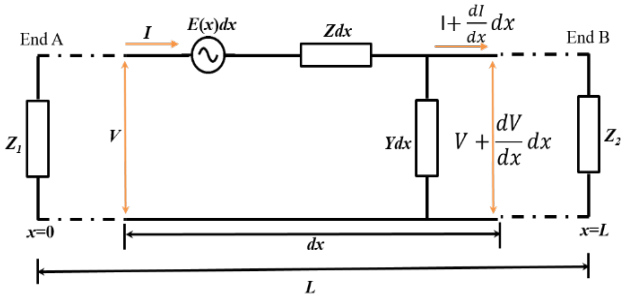

Fig. 3. An equivalent circuit of a buried pipeline with an inductive coupling from HVTL.

Considering Fig. 3, each pipeline incremental length dx may be described by its source potential $E(x)dx$ where $E(x)$ represents the longitudinal induced EMF on the pipe, derived in Section II-B. Z and Y denote the pipe longitudinal impedance and shunt admittance per unit length. The distributed potential and current along the pipeline incremental length may be obtained by solving the well-known transmission lines differential equations relating the quantities E, V and I as

$$\frac{d}{dx}V = E(x) - ZI(x) \tag{10}$$

$$\frac{d}{dx}I = -YV(x) \tag{11}$$

Substituting (11) into the derivative of (10) with respect to x, it is possible to write

$$\frac{d^2}{dx^2}V(x) = \gamma^2 V(x) + \frac{d}{dx}E(x) \tag{12}$$

In (12), γ represents the pipeline propagation constant (m^{-1}). Thus $\gamma = \sqrt{ZY}$.

The longitudinal induced EMF is constant under both steady state and fault conditions along the entire exposure length of the pipe, that is, $E(x) = E_p$. By considering a pipeline section which continues for some kilometres beyond ends A and B, the termination impedances Z_1 and Z_2 may be taken as being equal to the pipeline characteristics impedance seen from points A and B. Therefore, resolving the expressions represented by (12) using this hypothesis, the pipe-to-soil potential $V(x)$ along the pipeline section at any point x between zero and L, may be estimated as

$$V(x) = \frac{E_p}{2\gamma}\left(e^{-\gamma(L-x)} - e^{-\gamma x}\right) \tag{13}$$

For a buried coated pipeline, the longitudinal impedance Z and its shunt admittance Y per unit length may be estimated using (14) and (15) [28]

$$Z = \frac{1}{\pi D_p}\sqrt{\pi f \rho_p \mu_o \mu_p} + \frac{\pi f \mu_o}{4} + j\frac{1}{\pi D_p}\sqrt{\pi f \rho_p \mu_o \mu_p} + j\mu_o f ln\left(\frac{3.7}{D_p}\sqrt{\frac{\rho_{soil}}{2\pi f \mu_o}}\right) \tag{14}$$

$$Y = \frac{\pi D_p}{\rho_c t_c} + j\left(2\pi f \frac{\varepsilon_o \varepsilon_c \pi D_p}{t_c}\right) \tag{15}$$

where D_p denotes the pipeline diameter, ρ_p is the resistivity of the pipeline, μ_o is the permeability of free space usually expressed as $4 \times 10^{-7} H/m$, μ_p is the relative permeability of the pipe material, f is the operating frequency of the transmission line, ρ_c is the resistivity of the pipe coating material, ε_c is the relative permittivity of the pipe coating material and ε_o is the permittivity of free space expressed as $8.85 \times 10^{-12} F/m$.

D. The AC density estimation

As stated in earlier sections, the induced potential on the pipeline causes current circulation between the pipeline and the surrounding soil through a pipe coating defect. At the point of defect, the pipe has a resistance R to remote earth which may be expressed as

$$R = \frac{\rho_{soil}}{2D}\left[1 + \frac{8t_c}{D}\right] \tag{16}$$

where D represents the diameter of the defect. Using the traditional ohm's law relating the current, voltage and resistance, it is possible to write

$$I = \frac{2D^2 V_{ps}}{\rho_{soil}(D + 8t_c)} \tag{17}$$

Assuming a circular shape defect with surface area $A = \pi D^2/4$, the current density J through the defect may well be expressed as $J = I/A$. By further simplification, the AC density J_{ac}, through the defect at a point x along the length of the pipeline section may be expressed as

$$J_{ac} = \frac{8V(x)}{\pi \rho_{soil}(D + 8t_c)} \tag{18}$$

where $V(x)$ represents the pipe-to-soil potential at a point x, along the length of the pipeline section estimated earlier in Section II-C.

E. The relative risk value of AC corrosion estimation

The relative risk (RR) value of AC corrosion at any point x along the length of the pipeline buried in a soil may be expressed as

$$RR(x) = \frac{V(x)}{\rho_{soil}} \tag{19}$$

As may be observed, the above analysis is accomplished using the concept estimating the mutual impedances between the line conductors and the pipeline [29]. It is worthwhile to mention that for the sake of simplicity while still maintaining

generality without any noticeable technical error, the soil is assumed to be homogeneous with uniform soil resistivity. Also, the reciprocal effects of the earth wires on each other are neglected. Thereafter, a GUI was developed for these corrosion assessment criteria meant for AC induced corrosion risk monitoring and analysis.

F. GUI development and model evaluation

A MATLAB-based graphical user interface (GUI) was developed and made to run as a stand-alone application using the *deployment tool* in MATLAB, for monitoring the AC induced corrosion risk assessment indices. It eases the evaluation of the pipe-to-soil potential and the AC densities through a pipeline defect at any point on the pipe. The GUI displays result such as the induced voltage on the pipeline, the pipe-to-soil potential, the relative risk value of AC corrosion as well as the current density through a coating defect on the pipe based on the user input data from field measurement as may be observed in Fig. 4.

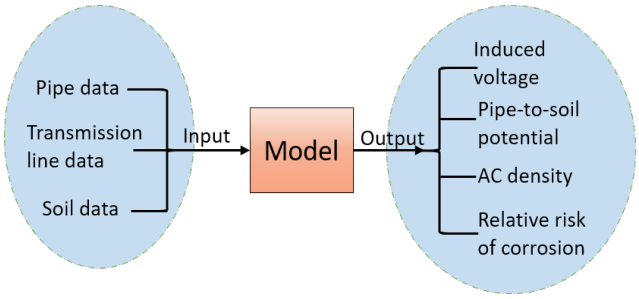

Fig. 4. The model input and output parameters.

Moreover, a flow chart illustrating the operation of the GUI-based AC induced corrosion risk assessment is illustrated in Fig. 5. From the start menu, the user supplies input data from field measurements and laboratory test to the input section of the interface. These data include the pipeline data, soil data and the transmission line data. Thereafter, the program computes the AC assisted corrosion risk assessment criteria shown in Fig. 5, based on the developed pipeline-to-transmission line model ROW. Since the AC density through a coating defect on the pipeline was acknowledged as the utmost criteria for assessing and predicting corrosion due to AC interference, this was selected by the program and its threshold value reported therein was mostly used for the pipeline corrosion risk assessment and monitoring purposes. More importantly, if the estimated AC density through the coating defect, after field input data by the user was greater than 100 A/m^2, the interface gives information on the AC corrosion condition on the pipeline in such site based on the supplied field data. Also, recommendations are given regarding the installation of a mitigation system. Other AC induced corrosion conditions due to the influence of the transmission line which may also occur on pipelines installed in such site are displayed on the chart in Fig. 5. The user may exit the program or vary the field input data to have a more varying output for detailed analysis of the pipeline AC corrosion conditions. A full detail of the pipeline-transmission line model derivation and the GUI step-by-step development may be found in [30].

III. Results and Discussions

The GUI displays result, such as the induced voltage on the pipeline, the pipe-to-soil potential, the relative risk value of AC corrosion as well as the current density through a coating defect on the pipe based on the user input data from field measurement. These AC corrosion risk assessment criteria may be monitored using the developed GUI to ensure that a threshold value above which there is a higher likelihood of corrosion damage to the pipeline is not exceeded. If in any case the threshold is exceeded, it will prompt the user to give adequate corrective measures through the installation of AC mitigation system or any other equivalent AC reduction strategies.

A. The developed GUI

The opening interface of the developed GUI is shown in Fig. 6. This displays among others, the title of the work, and the GUI developers. As may be observed in Fig. 6, clicking the start button from the file menu bar brings up Fig. 7, which shows the interface for the AC induced corrosion risk monitoring platform for the Rand Water Strydpan site based on the pipeline-transmission lines model ROW. As shown in Fig. 7, the interface consists of three input section for pipeline, soil and transmission line parameters. It also provides options for choosing the phase conductor transposition/combinations between the four transmission lines in that site to analyse its effect on the corrosion assessment criteria. Thereafter, a result section is provided featuring, among others, the longitudinal induced voltage and the AC density.

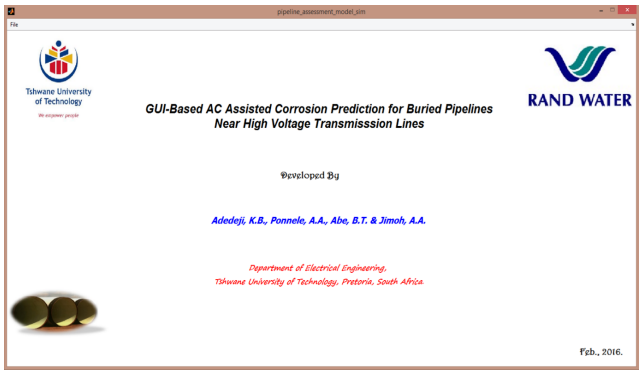

Fig. 6. The GUI opening interface.

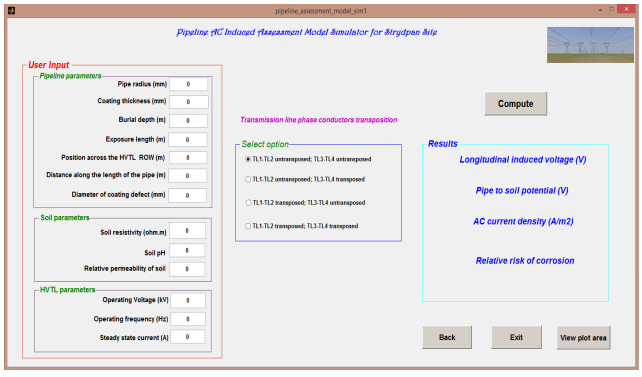

Fig. 7. Pipeline AC induced corrosion assessment window for the Strydpan site.

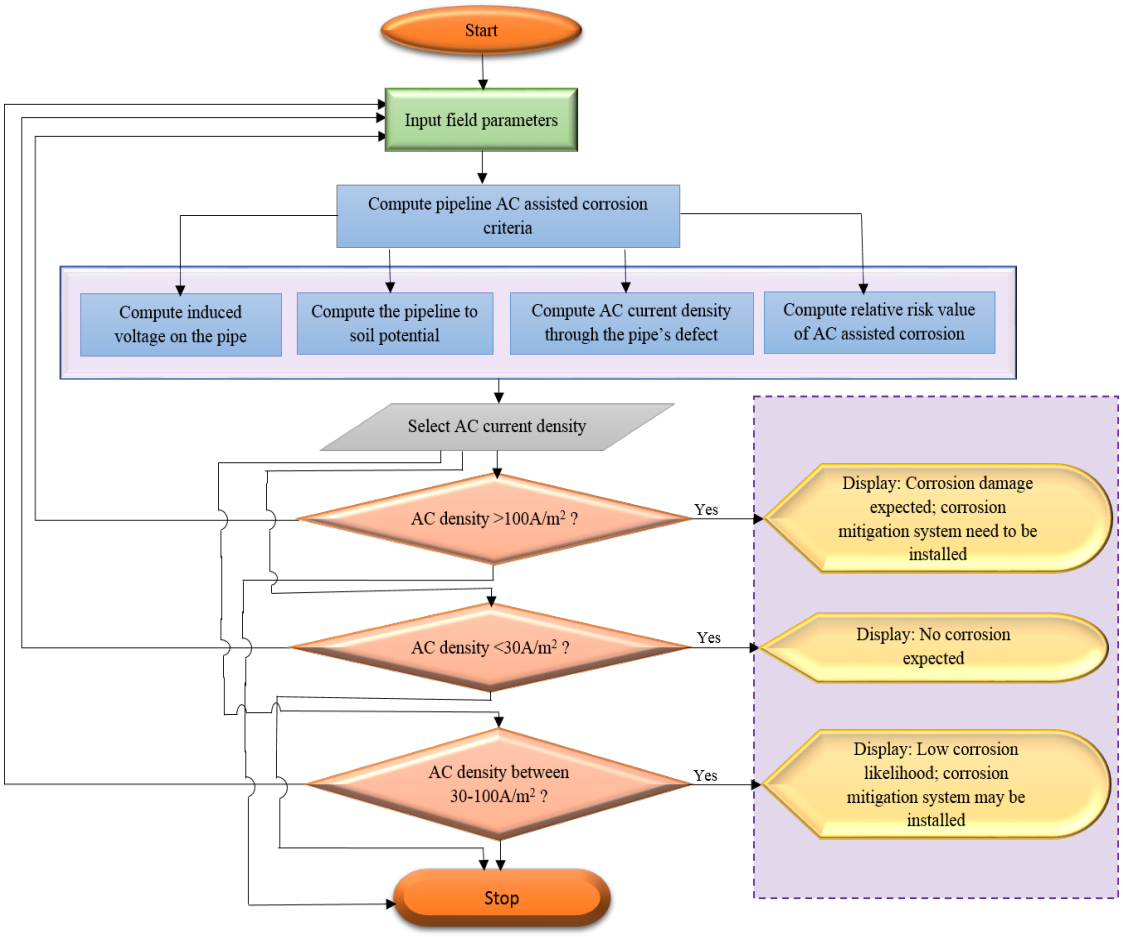

Fig. 5. An illustration of the developed GUI operation.

B. Running the GUI with user input data

To test the applicability of the developed GUI application, the data relating to the HVTL-pipeline in a real case study site where AC interference is frequent is shown in Table I and Table II. It is important to mention that experimental measurements in such site have shown that the soil can be assumed homogeneous with a measured soil resistivity of 12.96 Ωm. Table II shows the conductor rating of the HVTL in the case study site used for the program verification. The maximum rated current (maximum current capacity of the line conductors) of the transmission line conductors was applied as inducing current in accordance with Eskom guide [31]. In general, Zebra type conductor commonly used in South Africa for transmission line conductors, has a maximum current carrying capacity of 710 A at normal operating condition (Rate A) as illustrated in [31]. However, considering the transmission lines at case study site, the maximum MVA rating of the line at 275 kV is 676 MVA and 1353 MVA for two bundles (TL1 & TL2) and four bundles conductor (TL3 & TL4) respectively as shown in Table 2. Therefore, the line current is 410 A (rms) per conductor which is now the maximum current carrying capacity for the transmission line phase conductor at that site with operating voltage of 275 kV. This maximum current is used as inducing current in accordance with Eskom guide. This rated current was multiplied by the number of sub-conductors in the bundle. Hence for a line with two bundle conductors (TL1 & TL2), the rated current is 820 A and 1640 A for four bundle conductors (TL3 & TL4).

TABLE I
THE CASE STUDY PARAMETERS

S/N	Parameter	Value
1	Diameter	1000 mm
2	Burial depth	1 m
3	Defect size	1 mm
4	Exposure length	1000 mm
5	Coating thickness	4 mm
6	Soil resistivity	12.96Ωm
7	Soil relative permeability	1
8	Operating frequency	50 Hz
9	Operating voltage	275 kV
10	Peak load current per conductor	410 A

TABLE II
CONDUCTOR RATINGS OF THE HVTLS IN THE CASE STUDY SITE

HVTL ID	Number of conductors	Template Temperature (^oC)	Thermal rate A (MVA)	Thermal rate B (MVA)
TL1 & TL2	2	50	676	974
TL3 & TL4	2	50	676	974

The input data provided in Table I were supplied to the interface shown in Fig. 7. The presented GUI generates for the user defined boundary conditions of the HVTL-

pipeline right-of-way, the AC interference results based on the supplied input data from field measurements. Also, for more interference analysis, the application presents results for the effect of the phase conductor transpositions of the transmission lines in the study site on the induced potentials on the pipe. For the layout in Fig. 2, the phase conductor transposition has the following options:

1) TL1-TL2 phase conductors are un-transposed; TL3-TL4 phase conductors un-transposed:
2) TL1-TL2 phase conductors are un-transposed; TL3-TL4 phase conductors transposed:
3) TL1-TL2 phase conductors are transposed; TL3-TL4 phase conductors un-transposed:
4) TL1-TL2 phase conductors are transposed; TL3-TL4 phase conductors transposed.

Fig. 8 shows the features of the interface when the user input data was supplied before simulation. Fig. 9 shows the interface after simulation. In Fig. 8, a comment on the soil pH level in which the pipeline is buried is first provided by the interface. Looking at the figure, a message box displayed before simulation, the level of the corrosion threat of the supplied pH value of the soil to the pipeline. This gives a pre-warning on the corrosiveness of the surrounding soil where the pipe is buried. This information is meant to give the user an insight on the level of threat from the soil in which the pipeline is exposed. As may be observed in Fig. 8, a supplied pH value of 5.5 measured from the field, falls within the acidic medium, hence corrosive to the pipeline.

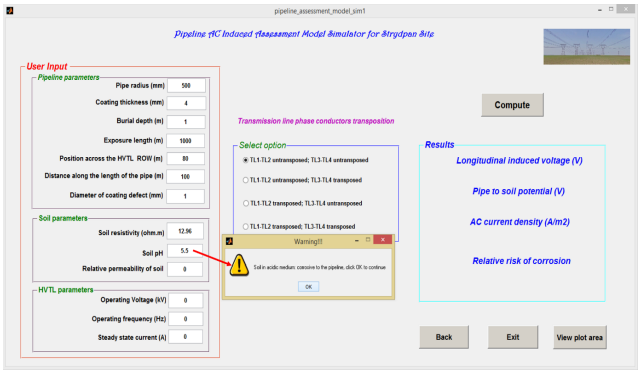

Fig. 8. Running the GUI with user input data displaying comment on the soil pH level.

Considering Fig. 9, the AC density through a 1 mm coating defect on the pipe, after simulation, is displayed. A message box also pop-up to display the comment on the level of AC density obtained through a 1 mm coating defect at a point 100 m along the length of the pipeline based on the supplied input. On the interface in Fig. 9, a threshold value of 100 A/m^2 above which a higher likelihood of corrosion damage is expected on pipelines has been exceeded. Consequently, the user knows the pipeline is exposed to corrosion damage at exactly 100 m along the parallel route. This then prompts for urgent action to be taken and AC corrosion mitigation strategies be deployed around that point.

Furthermore, in Fig. 10, the graphical user interface was used to display plots of the induced potential on the pipeline due to the inductive coupling effects from the four HVTLs. This may be accomplished by clicking the *view plot area*

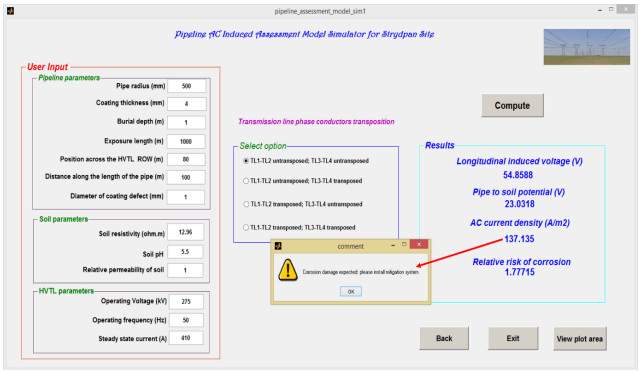

Fig. 9. The GUI displaying comment on the AC density after simulation.

button on the interface shown in Fig. 9, after supplying the input data. As may be observed in Fig. 10, by specifying the pipeline position across the transmission line right-of-way and choosing an option for the transmission line phase conductor transposition, for instance, TL1-TL2 phase conductors untransposed; TL3-TL4 phase conductors untransposed, and clicking the plot button, a plot of the longitudinal induced voltage on the pipeline with position across the transmission line is displayed. The plot also shows the effect of each of the four transmission lines. From the plot, the areas across the transmission line's route where the pipeline will experience higher induction from the line may be observed.

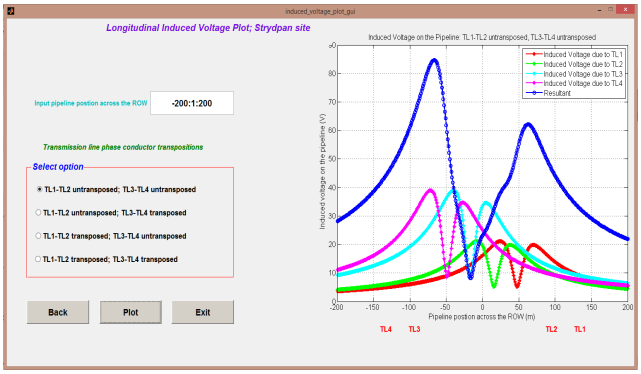

Fig. 10. The GUI displaying plot of longitudinal induced potential on the pipeline, with pipeline placed at different locations across the transmission line route for transmission line phase conductor transposition option of TL1-TL2 phase conductors untransposed; TL3-TL4 phase conductors untransposed.

Observing the profile of the induced potential on the pipeline, it may be observed that the maximum potential occurs on the pipe at some distance beyond the last phase conductors of the two extreme ends of the transmission lines. These two ends of the transmission lines (Fig. 2) corresponds to 57.2 m for the last phase conductor of TL1 and 58.05 m for that of TL4 in Fig. 10. Moreover, the Eskom guide for installing structures near a transmission line servitude in South Africa stated that no structure is permitted for 23.5 m for a 275 kV transmission line measured from the centre line of the transmission line [31]. However, the two extreme transmission lines have a centre line distance of 48 m and 48 m measured from the reference point as shown in Fig. 2. Therefore, using the Eskom requirement of placing structures, these points corresponds to 71.5 m for (TL1) and 71.5 m (for TL4) on Fig. 10. Looking at these two points, it

may be observed that for new pipeline installations along the transmission lines, pipelines installed near TL1, and away from this point (71.5 m) will experience lower induced potential compared to those installed near TL4. Thus, to reduce the induced potential on the pipe, when considering the option (1) of the phase conductor transposition, the pipe should be installed beside TL1 and with a minimum distance of 14.3 m from its last phase conductor.

In Fig. 11, a plot of the longitudinal induced potential on the pipeline with position across the transmission line is shown, by selecting the transmission line phase conductor transposition option TL1-TL2 phase conductors untransposed; TL3-TL4 phase conductors transposed from the interface in Fig. 10 and clicking the plot button. In a similar way to Fig. 10, one may observe areas across the transmission line's route where the pipeline will experience higher induction from the line.

Considering the profile of the induced potential in Fig. 11, it may be observed that there is a large reduction in voltage, especially on the other side of the transmission lines (TL4). It is obvious from the figure that pipelines installed near TL1 for these allowable distances (71.5 m away the centre line of the transmission lines) will experience much higher induced voltage than those installed near TL4. In general, it may be seen that the application through its interface may be used to assess the interference effect on a pipe installed in the right-of-way of a HVTL.

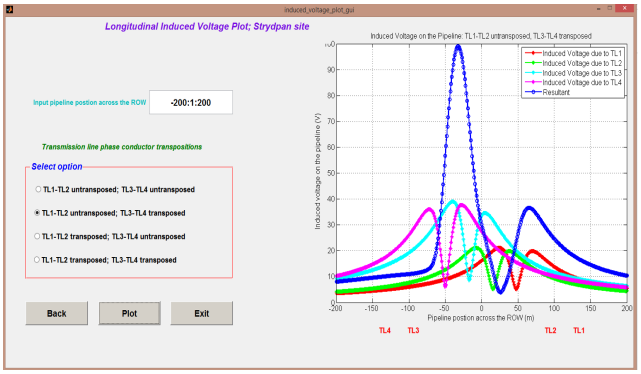

Fig. 11. The GUI displaying plot of longitudinal induced voltage on the pipeline with pipeline at different locations across the transmission line route for the transmission line phase conductor transposition option of TL1-TL2 phase conductors untransposed; TL3-TL4 phase conductors transposed.

IV. Conclusion

The development and implementation of a standalone graphical user interface of the AC induced corrosion risk assessment for monitoring the corrosion expectancies of a metallic pipeline buried near an existing transmission lines have been presented. The interface was developed using MATLAB software and has been tested to process user input data from field measurements in a Rand Water site in South Africa. This paper has shown how the developed GUI was used for evaluating the AC corrosion risk assessment indices based on the supplied input data. It can be inferred from the results presented that the interface is easy to use and provides a friendly user environment. Although, the application was developed to assess and monitor the corrosion expectancies in a Rand Water site, South Africa, improving the application for deployment in any situation of pipelines and transmission lines right of way remains a future research work.

References

[1] M.M. Saied, "The capacitive coupling between EHV lines and nearby pipelines," *IEEE Transactions on Power Delivery*, vol. 19, no. 3, 2004, pp. 1225-1231.

[2] J.P. Nelson, "Power systems in close proximity to pipelines," *IEEE Transactions on Industry Applications*, vol. 1A-22, no. 1, 1986, pp. 435-441.

[3] K.B. Adedeji, A.A. Ponnle, B.T. Abe, A.A. Jimoh, "Analysis of the induced voltage on buried pipeline in the vicinity of high AC voltage overhead transmission lines," *Proceedings of the 23rd Southern African Universities Power Engineering Conference*, 7-12, Johannesburg, 28-30th January, 2015.

[4] A. Ogunsola, A. Mariscotti, L. Sandrolini, "Estimation of stray current from a DC-electrified railway and impressed potential on a buried pipe," *IEEE Transactions on Power Delivery*, vol. 27, no. 4, 2012, pp. 2238-2246.

[5] M.O. Ouadah, O. Touhami, R. Ibtiouen, "Diagnosis of the AC current densities effect on the cathodic protection performance of the steel x70 for a buried pipeline due to electromagnetic interference caused by HVPTL," *Progress In Electromagnetics Research M*, vol. 45, 2016a, pp. 163171.

[6] M.O. Ouadah, O. Touhami, R. Ibtiouen, "Diagnosis of AC corrosion on the buried pipeline due to the high voltage power line," *Journal of Electrical Engineering*, vol. 16, 2016, pp. 76-83.

[7] G.C. Christoforidis, D.P. Labridis, P.S. Dokopoulos, "Inductive interference on pipelines buried in multilayer soil due to magnetic fields from nearby faulted power lines," *IEEE Transactions on Electromagnetic Compatibility*, Vol. 47, no. 2, 2005a, pp. 254-262.

[8] K. Kopsidas, I. Cotton, "Induced voltages on long aerial and buried pipelines due to transmission line transients," *IEEE Transactions on Power Delivery*, vol. 23, no. 3, 2008, pp. 1535-1543.

[9] L. Qi, H. Yuan, Y. Wu, X. Cui, "Calculation of overvoltage on nearby underground metal pipeline due to the lightning strike on UHV AC transmission line tower," *Electric Power Systems Research*, vol. 94, 2013, pp. 54-63.

[10] NACE RP0177, "Mitigation of alternating current and lightning effects on metallic structures and corrosion control systems," *NACE International Standard Practice*, Houston, Texas, 2007.

[11] S. Goidanich, L. Lazzari, M. Ormellese, "AC corrosion-part 1: effects on over-potentials of anodic and cathodic processes," *Corrosion Science*, vol. 52, no. 2, 2010a, pp. 491-497.

[12] CEN/TS12954, "Cathodic protection of buried or immersed metallic structures: general principles and application for pipelines," *European Technical Specification*, Germany, 2001.

[13] CEN/TS15280, "Evaluation of AC corrosion likelihood of buried pipelines-application to cathodically protected pipelines," *Technical Specification, CEN-European Committee for Standardization*, 2006.

[14] S. Goidanich, L. Lazzari, M. Ormellese, "AC corrosion. part 2: parameters influencing corrosion rate," *Corrosion Science*, vol. 52, no. 3, 2010b, pp. 916-922.

[15] S.D. Philip, "Overview of HVAC transmission line interference issues on buried pipelines," *Proceedings of the NACE Northern Area Western Conference*, Alberta, Canada, Feb. 15-18, 2010.

[16] A. Fu, Y. Cheng, "Effect of alternating current on corrosion and effectiveness of cathodic protection of pipelines," *Canadian Metallurgy Quarterly*, vol. 51, no. 1, 2012, pp. 81-90.

[17] M. Zhu, C. Du, X. Li, Z. Liu, S. Wang, J. Li, D. Zhang, "Effect of AC current density on stress corrosion cracking behaviour of X80 pipeline steel in high pH carbonate/bicarbonate solution," *Electrochimica Acta*, vol. 117, 2014, pp. 351-359.

[18] A. Brenna, L. Lazzari, M. Pedeferri, M. Ormellese, "Cathodic protection condition in the presence of AC interference," *La Metallurgia Italiana*, no. 6, 2014, pp. 29-34.

[19] M.H. Ouadah, M. Zergoug, A. Ziouche, O. Touhami, R. Ibtiouen, S. Bouyegh, C. Dehchar, "AC corrosion induced by high voltage power line on cathodically protected pipeline," *Proceedings of the International Conference on Control, Engineering and Information Technology*, Sousse, Tunisia, 22–25 March, 2014.

[20] D.Z. Tang, Y.X. Du, Y. Liang, M.X. Lu, Z.T. Jiang, "Electrochemical studies of the galvanic coupling zinc/pipeline steel in the presence of an applied alternating current," *Materials and Corrosion*, vol. 67, no. 5, 2016, pp.463–470.

[21] M.O. Ouadah, T.R.Ibtiouen, M.F. Benlamnouar, M. Zergoug, "Corrosive effects of the electromagnetic induction caused by the high voltage power lines on buried X70 steel pipelines," *International Journal of Electrical Power & Energy Systems*, vol. 91, 2017, pp. 34-41.

[22] K.B. Adedeji, A.A. Ponnle, B.T. Abe, A.A. Jimoh, A.M. Abu-Mahfouz, Y. Hamam, "AC induced corrosion assessment of buried pipelines near HVTLs: A case study of South Africa," *Progress in Electromagnetic Research B*, vol. 81, 2018, pp. 45-61.

[23] Y. Xiao, Y. Du, D. Tang, L. Ou, H. Sun, Y. Lu, "Study on the influence of environmental factors on AC corrosion behaviour and its mechanism," *Materials and Corrosion*, vol. 69, no. 5, 2018, pp.601–613.

[24] D.D. Micu, G.C. Christoforidis, L. Czumbil, "AC interference on pipelines due to double circuit power lines: A detailed study," *Electric Power Systems Research*, vol. 103, 2013, pp. 1–8.

[25] L. Czumbil, G.C. Christoforidis, D.D. Micu, D. Stet, A. Ceclan, A. Pop, "A user friendly software application for induced voltage evaluation," *Proceedings of the 46th International Universities Power Engineering Conference*, Soest, Germany, 5–8 September, 2011.

[26] Safe Engineering Services (SES) and Technologies Ltd., 1544 Viel, Montreal, Quebec, Canada. www.sestech.com.

[27] Low-Fi, Sigma Power Engineering Pty Ltd. www.sigmapower.com.au

[28] CIGRE, "Guide on the influence of high voltage AC power systems on metallic pipelines," CIGRE Working Group 36.02 Technical Brochure no. 095, 1995.

[29] J.R. Carson, "Wave propagation in overhead wires with ground return," *Bell System Technical Journal*, vol. 5, pp. 1926, 539-554.

[30] K.B. Adedeji, "Development of an assessment model and graphical user interface for monitoring alternating current interference induced corrosion of buried pipelines," *M.Tech Dissertation*, Department of Electrical Engineering, Tshwane University of Technology, Pretoria, South Africa, 2016.

[31] Eskom, "Guideline on the electrical co-ordination of pipeline and power lines," Paper No. 240- 66418968, pp. 2573, South Africa, 2015.